Non-Linear Modeling of Underwater Acoustic Waves Propagation for Multi-Receiver Channels

Pierre-Philippe J. Beaujean, Ocean Engineering Dept.
Andres A. Folleco, Computer Science & Engineering Dept.
Florent J. Boulanger, Ocean Engineering Dept.
Stewart A.L. Glegg, Ocean Engineering Dept.

Florida Atlantic University (FAU)
101 North beach Road
Dania Beach, FL, 33004, USA
pbeaujea@seatech.fau.edu

***Abstract*- A non-linear acoustic wave propagation model has been developed to determine the effects of ocean variations in the acoustic field, and to determine the signal measured by a receiver at any distance from an omni-directional source The model accounts for environmental conditions that include bathymetry, bottom properties, sound velocity profile and sea surface characteristics. First, a stationary estimate of the complex sound attenuation is computed as a function of frequency and location, using the parabolic equation numerical technique. For a given range, the vertical profile of the attenuation frequency spectrum is decomposed in the wave number domain. A specific Doppler shift is associated with each wave number. The space-frequency attenuation filter obtained is applied to the transmitted signal to create time-frequency selective fading. The non-linear acoustic wave propagation model has been specifically applied to the area of Port Everglades, Florida, to simulate the performance of the FAU General Purpose Acoustic Modem (FAU-GPAM). The modem operates in the 15.6 kHz to 31.9 kHz frequency band, with 192 dB of source level, and transmits Multi-Frequency-Shift-Key modulated sequences. The range of operation varied from 1 to 5 km, in 12 meters of water. The sea bottom is mainly composed of medium sand. Experimental data have been collected under sea-state 2 conditions. The performance of the acoustic communication system has been predicted using the non-linear model, the Crepeau model and experimental data. This work was sponsored by the Office of Naval Research, Code # ONR 321OM, Dr. Swean.**

I. INTRODUCTION

Acoustic communication in shallow water is made difficult primarily because of channel multipath. It arises from surface and bottom reverberations and geometric reflections from nearby objects such as piers, boats, in-water turbulence, thermal gradients, and other environmental factors.

A signal transmitted is severely limited by the transmission loss that increases non-linearly with both frequency and range. The bandwidth is typically inversely proportional to range and depends on environmental factors such as channel geometry, sea-state, temperature profiles, and ambient noise [2]. Within this limited bandwidth, W, the time-variant multipath depends highly on the location of the transmitter and receiver. While vertical channels tend to be affected little by multipath, horizontal channels may have very long multipath time spread, commonly in the order of hundreds of milliseconds. In underwater acoustic communications, multipath propagation causes Inter-Symbol Interference(ISI) [3].

The model can reproduce both time spread and Doppler spread effects to determine the signal measured by a receiver at any distance from an omni-directional source. A stationary estimate of the complex sound attenuation is calculated as a function of frequency and location, using the parabolic split-step equation numerical technique. This estimate is based on the Naval Research Laboratories Range-Dependent Acoustic Model (RAM) [4-6]. For the calculated range, the vertical profile of the attenuation frequency spectrum is decomposed in the wave number domain. A specific Doppler shift is associated with each wave number. The model makes the assumption that there is no relative movement between the source and the receiver nor does it consider Doppler shift is assumed to be caused only by surface wave motion.

The space-frequency attenuation filter obtained is applied to the transmitted signal to create time-frequency selective fading. The model performance is evaluated through a series of experiments at Port Everglades, south Florida. The region modeled ranges from 25.98 N to 26.2 N and from 80.8 W to 79.98 W. This area is known as the "South Florida Testing Facility (SFTF)".

II. TIME-DEPENDENT MODEL DESCRIPTION

A. *Frequency-Selective Fading*

Consider the acoustic transmission setup depicted in Fig. 1. A source, assumed to be omni-directional, transmits a broadband or narrow-band signal $x_T(t)$ in a shallow water acoustic channel. Assuming that the sea surface is flat, the modified Range-Dependent Acoustic Model (RAM) can be used to compute the complex attenuation coefficients at given location of the channel [5]. The environmental parameters required are the bathymetry $z_b(x)$, the sediment mass density ρ_b, the compressional wave velocity c_b of the sediment, and the sound velocity profile In order to simplify the problem, it is assumed that sound velocity profile and sediment characteristics are not range-dependent.

The spectrum $x_T(f)$ of the transmitted signal occupies a bandwidth W in the frequency domain, defined as a series of M frequency intervals of bandwidth Δf, centered around the frequency f_m , where m is an integer and $1 \le m \le M$. Let $R(x_R,z_R)$ be the receiver location and the vertical complex attenuation profile be $\widehat{\alpha}_{RAM,n,m}$ computed at points $R_n(x_R,z_{R,n})$, for a given frequency f_m using RAM, where n is an odd integer in $1 \le n \le N$ [5].

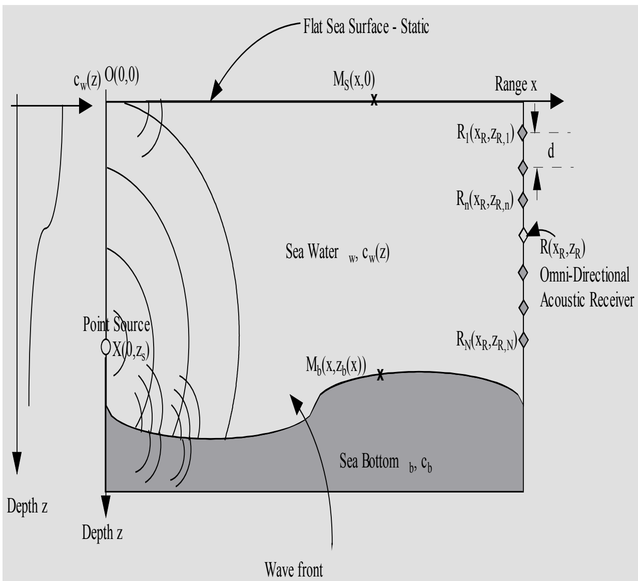

Fig. 1 Acoustic Transmission in Shallow Waters

The N points R_n are equally spaced d_m meters apart. The spacing d_m is a function of the frequency of operation:

$$d_m = \frac{\lambda_m}{\delta} = \frac{c}{\delta \times f_m} \tag{2.1}$$

where δ is an even integer, $\delta \ge 2$. The attenuation loss coefficients do not include the energy absorption due to viscous flow and chemical reactions. The loss due to absorption is calculated separately. Consider the absorption coefficient $a(f_m)$ in dB/m, [2]. Assuming an average water depth significantly smaller than the range and that wave refraction is small, the absorption loss $TL_{absorption}$ is approximately equal to:

$$TL_{absorption}(f_m) = a(f_m).x_R \; dB \tag{2.2}$$

The attenuation $\widehat{\alpha}_{n,m}$ computed at points $R_n(x_R,z_{R,n})$ can be approximated as:

$$\widehat{\alpha}_{n,m} = \widehat{\alpha}_{RAM,n,m} \cdot 10^{-\frac{(a(f_m)\,x_R)}{20}} \tag{2.3}$$

B. Spatial Decomposition

Since the estimate given in (2.3) is not time-dependent, $\widehat{\alpha}_{n,m}$ represents the complex frequency selective fading at the location $R_n(x_R,z_{R,n})$, as a function of the frequency f_m. Under the assumption of equal spacing of the points R_n, this vertical profile of the attenuation frequency spectrum can be decomposed in the wave number domain, as depicted in Fig. 2.

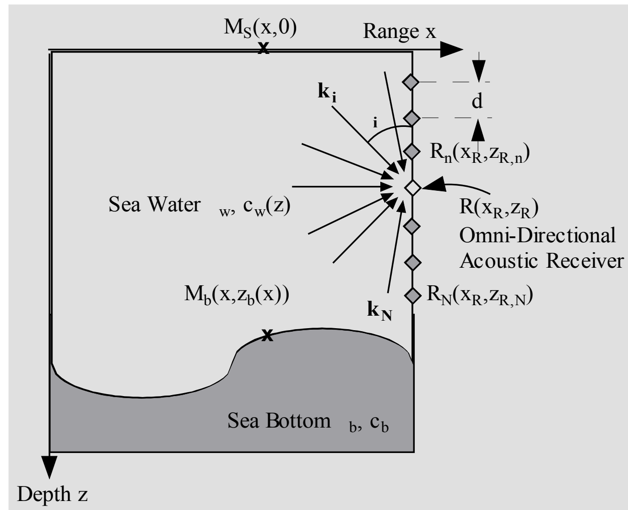

Fig. 2 Wave Number Decomposition along the Vertical Attenuation Profile

Assuming that wave refraction is small within the shallow water acoustic channel and under the plane wave approximation, each wave number $\vec{k}_i$ can be associated with an impact location over the sea surface or the sea bottom. This location is derived from the angle of arrival ϕ_i, where i is an integer and $1 \le i \le N$. The projection of the wave number $\vec{k}_i$ onto the vertical axis is expressed as:

$$k_{z,i} = \left\|\vec{k}_i\right\| \sin\phi_i \tag{2.4}$$

The fading spectrum $\hat{\alpha}(z,f)$ can be expressed analytically as a function of k_z and f using a Fourier Transform [7]:

$$\hat{\zeta}(k_z,f) = \int_{z_{R,1}}^{z_{R,N}} \hat{\alpha}(z,f) e^{-j2\pi k_z z} dz \tag{2.5}$$

$\hat{\zeta}(k_z,f)$ can be numerically represented as $\hat{\zeta}_{i,m}$, the complex fading at frequency f_m at the angle of arrival ϕ_i . Given a transmitted signal spectrum $X_T(f)$, the signal measured at the receiver location $R(x_R,z_R)$ for a given direction of arrival ϕ_i , associated with the wave number $k_{z,i}$, is:

$$X_{FSF}(f,k_{z,i}) = X_T(f).\zeta(k_{z,i},f) \tag{2.6}$$

C. Time-Selective Fading

The next step is to apply an individual Doppler shift to the faded signal $X_{FSF}(f, k_{z,i})$ associated with a specific direction of arrival ϕ_i:

$$X_{BL}(f, k_{z,i}) = G(f, k_{z,i}, X_{FSF}(k_{z,i}, f)) \tag{2.7}$$

The *BL* index indicates that the output spectrum is now subject to time-spread and Doppler-spread. The function $G(f, k_{z,i}, X_{FSF}(k_{z,i}, f))$ represents the Doppler shift operation, function of the frequency *f*, the direction of arrival ϕ_i and the faded signal spectrum $X_{FSF}(k_{z,i}, f)$. The motion of the sea-surface is assumed to be the only significant source of time-selective fading was done for simplification. In an effort to further simplify the problem, we assumed that only the $N_{Surface}$ directions of arrival ϕ_i corresponding to a sea-surface impact are subject to individual Doppler shifts. Using the index convention shown in Figure 2, the faded signal matrix $X_{FSF}(f, k_z)$ is split into two sub-matrices:

$$X_{BL}(f, k_z) = \begin{bmatrix} X_{BL}(f, k_{z,i}) & \{i = 1,.., N_{Surface}\} \\ X_{FSF}\left(f, k_{z,\, i+N_{surface}}\right) & \{i = 1,.., N - N_{Surface}\} \end{bmatrix} \tag{2.8}$$

From a numerical point of view, time operations are better suited to apply Doppler shifting to a time signal. Consider the analytical faded signal $\tilde{x}_{FSF}(t, k_{z,i})$ associated with a specific direction of arrival ϕ_i:

$$\tilde{x}_{FSF}(k_{z,i}, t) = \int_{-\infty}^{\infty} X_{FSF}(k_{z,i}, f).e^{j2\pi ft} df \tag{2.9}$$

In the case of a signal coming from the surface, the Doppler-shifted time signal is:

$$\tilde{x}_{BL}(k_{z,i}, t) = \tilde{x}_{FSF}(k_{z,i}, (1 + \Delta f_i(f)).t) \tag{2.10}$$

where $\Delta f_i(f)$ is the frequency shift associated with the surface motion in the direction specified by ϕ_i, and is a function of the surface velocity vector $\vec{U}_i$ at the impact location, as illustrated in Fig. 3:

$$\Delta f_i(f, \vec{U}_i) = \frac{U_i \cos\psi_i}{c_w} f \tag{2.11}$$

Based on environmental conditions, several models can be used to define the surface shape $M_s(x_s(t), z_s(x_s(t)))$ and the complex velocity $\vec{U}(x_s(t), z_s(x_s(t)))$. Details and justification for the model selection are presented in section *E,* [10].

D. Signal Reconstruction

The signal received at the hydrophone center location of the virtual array $R(x_R, z_R)$ is:

$$x_R(t) = n(t) + \Re\{\sum_{i=1}^{N_{Surface}} \tilde{x}_{BL}(k_{z,i}, t) + \sum_{i=1+N_{Surface}}^{N} \tilde{x}_{FSF}(k_{z,i}, t)\} \tag{2.12}$$

This is accomplished through the sum of the attenuated time signal corresponding with each direction of arrival ϕ_i. The model has the assumption that the ambient noise is isotropic. The scaled ambient noise *n(t)* is a Gaussian random sequence $G(0,1)$ of zero-mean and unit standard deviation, filtered by a designated noise Power Spectral Density function $N_o(f)$:

$$n(t) = \int_{-\infty}^{\infty} \left(\int_{-\infty}^{\infty} G(0,1)\, e^{-j2\pi ft} dt \right) . N_o(f)\, e^{j2\pi ft} df \tag{2.13}$$

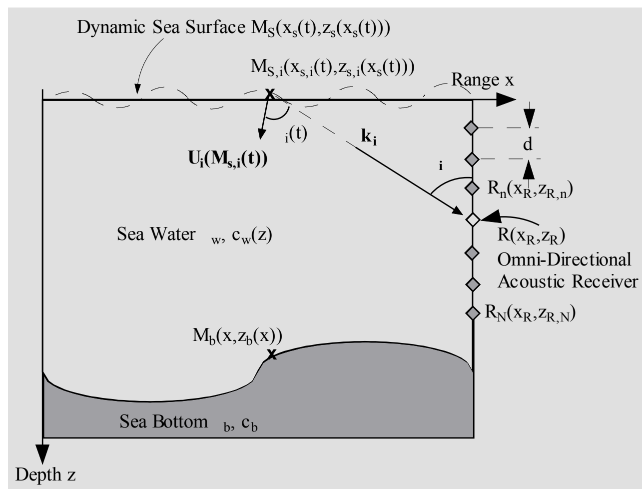

Fig. 3 Doppler Shift due to Surface Dynamics

E. Surface Wave Model

Ocean surface waves are seen as a superposition of random waves of various lengths and periods with different frequencies ω_i, each with corresponding amplitude A_i and phase Φ_i. The spectrum represents the distribution of wave energy amongst different wave frequencies of wave lengths on the sea surface [10]. The 2-D model presented here is describing wind-generated waves in a fully-developed sea. For simplicity, a wave spectrum with one peak frequency is considered, but with properly chosen parameters of the model, a realistic situation of the swell from one storm interacting with the waves from another storm can be obtained. The development of the model focused on the Pierson spectrum, a commonly adapted spectrum for the location of the experiment [10]. Pierson and Moskovitz

(PM) [10] developed a wave spectral formulation for fully developed wind-generated seas from analyses of wave spectra in the North Atlantic Ocean. The PM spectrum is written as:

$$S(\omega) = A \cdot \omega^{-5} \cdot \exp\left(-B\omega^{-4}\right) \ldots\ldots\ldots \left[\frac{m^2}{s}\right] \tag{2.14}$$

where $A = 8.1 \cdot 10^{-3} \cdot g^2$ and $B = 0.74 \cdot \left(\frac{g}{V}\right)^4$

V the wind speed in knots at a height of 19.4 m over the sea surface and g is the gravity constant. By assuming that the waves can be represented by Gaussian random processes and that $S(\omega)$ is narrow-banded, the PM-spectrum can be reformulated in terms of significant wave height, that is [10]:

$$A = 8.1 \cdot 10^{-3} \cdot g^2 \text{ and } B = 0.0323 \cdot \left(\frac{g}{H_S}\right)^2 = \frac{3.11}{H_S^2} \tag{2.15}$$

III. EXPERIMENTAL PROCEDURE

The model results were compared to experimental data obtained near Fort Lauderdale, Florida. Two FAU acoustic modems were placed at 6 meter depths with bottom depth at 12 meters. The Mills-Cross vertical array [11] was used as a second receiver. The receivers were stationary and controlled from the ship R/V Stephan. The source was moving away (by the R/V Lee) up to 5 km from the receivers. Transmissions occurred under operating conditions that included boat(s) and ambient noise, and a small steady Doppler shift component caused by the vessel motion (0 to 5 knots). Five acquisitions were made (10 under the wide-sense stationarity assumption for two receivers) for the four transmission modes (with 8 synchronization pulses) of the acoustic modem. Biological activity and boat traffic was fairly high, with a measured background noise PSD level of $57\, dB\, re\, 1\, \mu Pa / \sqrt{Hz}$, linearly averaged between 16 kHz and 32 kHz. The noise Power as a function of the frequency in a 295.31 Hz bandwidth of the first incoming symbol, carrying a frequency $f_1 = 24.5\ kHz$ was measured. Source operated with 192 dB of source level and used Multi-Frequency-Shift-Key (MFSK) modulated sequences. For more details on the acoustic communication system, the reader can refer to reference [9], published in the same conference proceedings.

For a given time and location, the surface elevation $\eta(x, y, t)$ is computed using the inverse Fourier transform of $S(\omega)$ and the random phase parameter. The wind speed was set to 15 knots to simulate experimental conditions and obtain wave heights of up to 1 m. The wave shape is calculated at every point of impact (x and y positions and velocities) with the signal directions at the times corresponding to each symbol. Complex attenuation losses were obtained for 64 frequencies per band number with the acoustic modems using 56 band numbers of 295.3 Hz bandwidth each for a total of 3584 frequencies from 15.6 to 32.1 kHz. The experiment area's bathymetry is mostly reef and coarse sand which results in a highly reverberant environment. Sediment/reef sound speed was set to $c_{bottom} = 1650\, m/s$ and sediment acoustic impedance $\rho_{bottom} = 2.07\, g/cm^3$.

Conductivity, Temperature and Density measurements revealed minimal depth dependency which implied the presence of an isospeed channel. The vertical resolution of the attenuation loss grid should be the distance desired between 2 virtual receivers $d_m = \frac{\lambda_m}{\delta} = \frac{c}{\delta \times f_m}$ and it has to be set to a maximum of $\frac{\lambda}{2}$ for efficiency of the array as a spatial filter. The space factor was increased to 4 in order to improve the accuracy of the model.

After some tests, the horizontal resolution was set to 0.5 meter. By comparing attenuation losses that do not account absorption with those that do, the losses increased from 2.6 dB at 1 km to 13.1 dB at 5 km. Figs 4 and 5 show that due to absorption the attenuation losses are frequency-dependent (the higher the frequency, the higher the loss). The attenuation losses were decomposed in wave numbers to obtain $\zeta(f)$.

IV. RESULTS

The system was reverberation limited at less than 3km and noise limited beyond that range. These effects worsened for transmission modes 1, 2, and 3 because of less allocated energy per frequency band [9] [12]. Fig. 6 shows that the model tends to over estimate the number of errors at the fastest modes, mode 1 in particular. The model

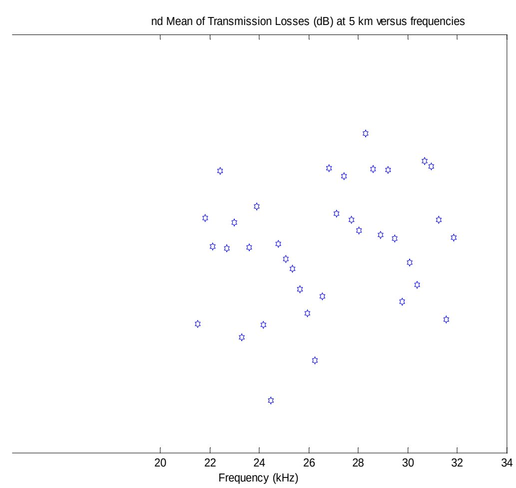

Fig. 4 Transmission Loss at 5km (No Absorption)

creates larger amounts of reverberation than the actual acoustic field because it assumes that both source and receiver are omnidirectional. In reality, Bernault [12], Jacquemin [13] and Beaujean [11] have shown that the modem source and the MillsCross receiver are not perfectly omni-directional. Directivity at the source will naturally reduce the reverberation time through the channel, while a directive receiver will act as a spatial filter. The model predictions were also compared with the results obtained from Crepeau model [12,14], as shown in Table 1. The Frame Error Rate (FER) associated with mode 4 as a function of range using one channel. The FER simply corresponds to the percentage of message properly decoded during a series of messages transmission.

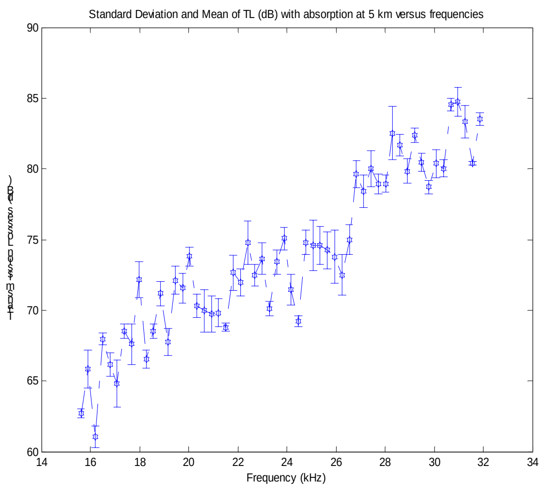

Fig. 5 Transmission Loss with Absorption at 5km

The Crepeau model can be fairly accurate over thousands of trials. Our model performs fairly at close range (1-2 km), but tends to overestimate the modem performance at further ranges (3-5 km). This confirms that the ambient noise level may have been somewhat underestimated during transmission in mode 4 at 5 km.

TABLE 1 NAKAGAMI M-COEFF. AND CREPEAU FER DISTANCE DEPENDANCE

Range (km)	**ML (m)**	**FER (%)**
1	**5.3876**	**3**
2	**3.5791**	**13**
3	**4.7027**	**15**
4	**2.8350**	**23**
5	**4.8130**	**29**

V. CONCLUSION

A novel underwater acoustic wave propagation model enables the determination of the signal measured by a receiver at any distance from an omni-directional source in very shallow water. The performance of the time-dependent model improves with increasing mode number and decreasing range, as the energy per symbol increases and the maximum reverberation time tolerated increases with the mode number. When varying the two random parameters, ambient noise and phase generators of the surface wave model, the changes of the surface Doppler shift with time and space cause as much variation in the system's performance as instantaneous noise does. By comparing the model demodulation results to those obtained when decoding experimental signals, the model predicts the communication performance of FAU's acoustic modem. However, the model tends to overestimate the number of errors at the fastest modes, mode 1 in particular. The model creates larger amounts of reverberation than the actual acoustic field because it does not consider directivity. It has been shown that the modem source and the MillsCross receiver are fairly directive and will naturally reduce the reverberation time through the channel, while a directive receiver will act as a spatial filter. As suggested by the results, an important research topic is to apply the directivity of the source to the model and to improve the estimation of the ambient noise added to the signals simulated by the model.

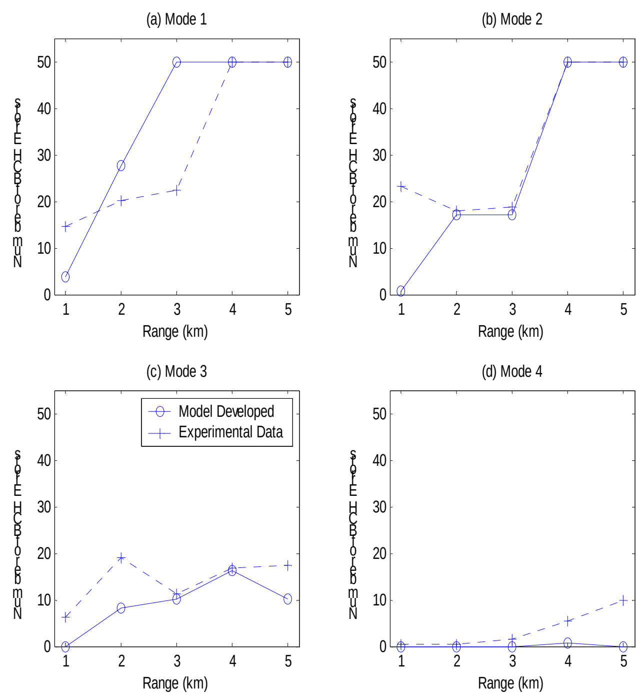

Fig. 6 Signal Demodulation Results

References

[1] R.J. Urick, *Principles of Underwater Sound,* 3rd ed., Peninsula Publishing, 1983.

[2] L.E. Kinsler, A.R. Frey, A.B. Coppens, and J.V. Sanders, *Fundamentals of Acoustics,* 4th ed., John Wiley & Sons, Inc., 2000.

[3] H.K. Yeo, B.S. Sharif, A.E. Adams, and O.R. Hinton, *Analysis of Experimental Shallow Water Network Channel and Theoretical Channel Model,* University of New Castle upon Tyne, UK, 1999.

[4] M.D. Collins, "A split-step Pade solution for the parabolic equation method," *The Journ. of Acoust. Soc. Of America,* 93(4), pp. 1736-1742, April 1993.

[5] M.D. Collins, "A two-way parabolic equation for elastic media," *The Journ. Of the Acoust Soc of America,* 93(4), pp. 1815-1825, April 1993

[6] M.D. Collins, "A self-starter for the parabolic equation method," *The Journ. Of the Acoust Soc of America,* 92(4), Pt. 1, October 1992.
[7] W.S. Burdic, *Underwater Acoustic System Analysis,* Beamforming chpt., Prentice Hall, 1991
[8] C. Ifeador and B.W. Jervis, *A Practical Approach to Digital Signal Processing,* 2rd ed., Prentice Hall, 2002.
[9] P. Beaujean and E. Bernault, "A new multi-channel spatial diversity technique for long range acoustic communications in shallow water," *Conf. Proc. Of IEEE Oceans 2003,* in press.
[10] E.V. Lewis, *Principles of Naval Architecture – Motions in Waves and Controllability.* Society of Naval Architects, 2nd ed, June 1990.
[11] P.P. Beaujean, *High-Speed Acoustic Communication in Shallow Water using Spatio-Temporal Adaptive Array Processing* . PhD Dissertation, Dept. of Ocean Eng.,Florida Atlantic University, 2000.
[12] E.P. Bernault, *Array Procesing Techniques for Frequency Hopping Multiple Frequency Shift Keying Long Range Communications.* M.S. Thesis, Dept. of Ocean Eng., Florida Atlantic University, 2002.
[13] J.P. Jacquemin, *Transducer Design for Underwater Acoustic Communications using Finite Element Method.* M.S. Thesis, Dept. of Ocean Eng., Florida Atlantic University, 2001
[14] R.L.Peterson, R.E. Ziemer, and D.E. Borth, *Introduction to Spread Spectrum Communications,* Prentice Hall, 1995.